Molecular Modeling Targeting the ACE2 Receptor with *Cannabis sativa*'s Active Ingredients for Antiviral Drug Discovery against SARS-CoV-2 Infections

Zainab El Ouafi[1], Wajih Rhalem[2], Nihal Habib[1], Abdellah Idrissi Azami[1], Sofia Sehli[1], Najib Al Idrissi[3], Fadil Bakkali[4], Rfaki Abderrazak[5], Mohamed Merzouki[6], Imane Allali[7], Saaïd Amzazi[7], Chakib Nejjari[8,9] and Hassan Ghazal[1,2,5]

[1]Laboratory of Genomics and Bioinformatics, School of Pharmacy, Mohammed VI University of Health Sciences Casablanca, Casablanca, Morocco. [2]Electronic Systems, Sensors and Nanobiotechnologies (E2SN), École Nationale Supérieure des Arts et Métiers (ENSAM), Mohammed V University, Rabat, Morocco. [3]Department of Surgery, School of Medicine, Mohammed VI University of Health Sciences Casablanca, Casablanca, Morocco. [4]Toxicology Laboratory, School of Medicine, Mohammed VI University of Health Sciences (UM6SS) Casablanca, Casablanca, Morocco. [5]National Center for Scientific and Technical Research (CNRST), Rabat, Morocco. [6]Bioengineering Laboratory, Faculty of Science and Technologies, University of Sultan Moulay Slimane, Beni Mellal, Morocco. [7]Laboratory of Human Pathologies Biology, Department of Biology, Faculty of Sciences, and Genomic Center of Human Pathologies, Faculty of Medicine and Pharmacy, Mohammed V University in Rabat, Rabat, Morocco. [8]Department of Epidemiology and Biostatistics, International School of Public Health, Mohammed VI University of Health Sciences Casablanca, Casablanca, Morocco. [9]Department of Epidemiology and Public Health, Faculty of Medicine, University Sidi Mohammed Ben Abdellah, Fes, Morocco.

ABSTRACT: The emergence of a novel coronavirus that later on rendered a global pandemic, caused desperation within the communities and drove increased interest in exploring medicinal plant–based therapeutics to treat and prevent severe acute respiratory syndrome coronavirus 2 (SARS-CoV-2) virus infections. Many medicinal plants have been reported to have antiviral, anti-inflammatory, and immunomodulatory effects that hinder, cure, or ease the symptoms of COVID-19 infection. This exploratory study seeks to dock the active components of *Cannabis sativa*, a natural plant with several pharmacological and biological properties, with the angiotensin-converting enzyme II (ACE2) receptor. A total of 3 *C. sativa* active components have been found to bind to the ACE2 protein active site and could inhibit spike binding, although they do not compete directly with the receptor-binding domain (RBD) of SARS-CoV-2. 6-Prenylapigenin, cannabivarin (CBN-C3), and Δ8-tetrahydrocannabinolic acid-A (Δ8-THCA) have a greater affinity (−8.3, −8.3, and −8.0 kcal/mol, respectively) and satisfactory interaction with ACE2 than its inhibitor MLN-4760 (−7.1 kcal/mol). These potential drugs with higher affinity for the ACE2 receptor and adequate absorption, distribution, metabolism, excretion, and toxicity (ADMET) values are candidates for treating or preventing SARS-CoV-2 infections. In vitro and in vivo investigations are needed to evaluate further the efficacy and toxicity of these hit compounds.

KEYWORDS: Medicinal plant, *Cannabis sativa*, COVID-19, SARS-CoV-2, ACE2, spike, drug discovery, molecular docking, ADMET

Introduction

Coronaviruses (CoVs) belong to the *Coronaviridae* family, and contain a positive-sense, single-stranded RNA genome. They are a substantial public health risk.[1] Coronavirus disease 2019 (COVID-19) is induced by severe acute respiratory syndrome coronavirus 2 (SARS-CoV-2), a recently identified CoV, causing a global pandemic. Human angiotensin-converting enzyme II (ACE2) acts as the receptor for severe acute respiratory syndrome CoVs SARS-CoV and SARS-CoV-2. The receptor-binding domain (RBD) of the CoV spike (S) protein, which is situated in the amino-terminal region (amino acids 318-510), is directly implicated in binding to ACE2.[2] Angiotensin-converting enzyme II (approximately 120 kDa) contains 4 parts: an N-terminal signal peptide, a C-terminal intracellular domain, a transmembrane domain, and a catalytic extracellular domain having a single metalloproteinase active site with a consensus HEXXH zinc-binding sequence domain in which 2 histidine residues chelate a catalytic zinc ion.[3] Angiotensin-converting enzyme plays an important role in the renin-angiotensin system (RAS).[4] However, despite many efforts, the dynamics and functional mechanism of the ACE2 receptor are still poorly understood.[5] To date, no novel medicine has been developed specifically for the treatment of COVID-19. It was demonstrated that many medicinal plants might lessen fever duration and provide symptomatic relief owing to their antiviral, immunomodulatory, and anti-inflammatory properties, which alleviate the symptoms of individuals suffering from COVID-19 infection.

Table 1. List of cannabinoid classes identified in *C. sativa*.[8]

CANNABINOIDS CLASS	NUMBER OF COMPOUNDS
(–)-trans-Δ9-tetrahydrocannabinol	18
(–)-trans-Δ8-tetrahydrocannabinol	2
Cannabigerol	17
Cannabichromene	8
Cannabidiol	8
Cannabinodiol	2
Cannabielsoin	5
Cannabicyclol	3
Cannabinol	10
Cannabitiol	9
Miscellaneous	22

Cannabis is a widespread plant that may be found in a broad range of environments and altitudes. Moreover, it is one of the oldest plants exploited as a food source and textile fabric source.[6] Cannabis cultivation extends back to the 17th century in Morocco, notably in the central Rif mountain, in the north of the country.[7] *C. sativa* contains 104 cannabinoids, categorized into 11 classes (Table 1), and 126 noncannabinoid components belonging to 8 distinct chemical classes: Flavonoids, Steroids, Phenanthrenes, Fatty acids, Spiroindans, Nitrogenous compounds, Xanthones, and Biphenyls.[8–10]

Several therapeutic possibilities, including repurposed pharmaceuticals and ab initio compounds, have been presented, such as MLN-4760, a cell-permeable, highly selective, and potent inhibitor (IC50 = 0.44 nM) of the ACE2 receptor.[11] MLN-4760 binds to the protein active site, which impedes natural substrate binding and inhibits the N-terminal catalytic peptidase domain (PD) of ACE2. The binding of MLN-4760 causes the receptor to establish a closed conformation in which the protein's active site is closed from the external environment.[12] *C. sativa* components could bind to the protein active site of ACE2 and inhibit substrate binding, thus preventing SARS-CoV-2 infection. In this article, we evaluated, through molecular docking and absorption, distribution, metabolism, excretion, and toxicity (ADMET) studies, the potential of these components to be used as ACE2 inhibitors and therefore as drug candidates to treat or prevent COVID-19.

Materials and Methods

Virtual screening was used to verify the major compounds with a higher affinity than the MLN-4760 inhibitor of ACE2. A total of 43 molecules of *C. sativa* were retrieved from the PubChem database, namely, Δ9-tetrahydrocannabinolic acid-A (THCAA) CID:98523, Δ9-tetrahydrocannabinolic acid-B

(THC-B) CID:46889976, tetrahydrocannabivarin (THCV) CID:93147, Δ8-tetrahydrocannabinol (Δ8-THV) CID:2977, Δ8-tetrahydrocannabinol acid-A (8-THCA) CID:59444391, Cannabigerol (CBG-C5) CID:5315659, Cannabigerolic acid (CBGA) CID:6449999, Cannabigerolic acid monomethyl ether (CBGAM) CID:24739091, Cannabigerovarin (CBGV) CID:59444407, Cannabigerovarinic acid (CBGVA) CID: 59444383, Cannabichromenic acid (CBCA) CID:3084339, Cannabichromevarin (CBCV) CID:6451726, Cannabichromevarinic acid (CBCVA) CID:11110322, Cannabidiolic acid (CBDA) CID:160570, Cannabidivarin (CBDV) CID: 11601669, Cannabidiol monomethyl ether (CBDM) CID: 164905, Cannabidivarinic acid (CBDVA) CID:59444387, Cannabimovone CID:46217279, Cannabinodiol (CBND-C5) CID:11551346, Cannabielsoin (CBE-C5) CID:162113, Cannabielsoic acid a (CBEA-C5) CID:59444405, Cannabielsoic acid-B (CBEA-C5B) CID:59444401, Cannabicyclol (CBL) CID:30607, Cannabicyclolic acid (CBLA) CID:71437560, Cannabinolic acid (CBNA) CID:3081990, Cannabivarin (CBN-C3) CID:622545, Cannabiorcol (CBN-C4) CID:22805649, Cannabinol-C2 (CBN-C2) CID:2543, (–)-trans-cannabitriol (CBT-C5) CID:156460, Cannabichromanone-B CID:186690, 2-geranyl-5-hydroxy-3-*n*-pentyl-1,4-benzoquinone CID:44139743, Cannabioxepane (CBX) CID:53309045, Chrysoeriol CID:5280666, 6-prenylapigenin CID:10382485, Acetyl stigmasterol CID:129671096, Alfa-spinasterol CID: 14237817, Daucosterol CID:5742590, 4,7-dimethoxy-1,2,5-trihydroxyphenanthrene CID:25172438, 9,10-dihydro-2,3,5,6-tetramethoxyphenanthrene-1,4-dione CID:129861810, 7-methoxycannabispirone CID:162936, Isocannabispiradienone CID: 10105874, Uracil CID:1174, and Cannabisin CID:15086398.

The ACE2 receptor was retrieved from the protein database (PDB) under the accession ID: 6VW1. Molecular docking was used to study the binding difference between *C. sativa* molecules and the MLN-4760 (CID: 448281) compound as a reference. Molecular visualization was performed with PyMOL[13] and Discovery Studio Visualizer (DSV).[14] The SwissADME server[15] was used to predict molar refractivity, saturation, and promiscuity for the leader compounds, and screening was performed using standard medicinal chemistry criteria offered by the tool. pkCSM[16] was used to screen for absorption, distribution, metabolism, elimination, and toxicity (ADMET) characteristics.

Molecular docking

Prior to testing the ligands against the SARS-CoV-2 target protein ACE2, the structures of the small molecules and the targeted protein were optimized using AutoDock Tools.[17] Molecular docking experiments were performed using PyRx.[18] To set the boundaries of the docking, we used grid box values of the ACE2 protein that were centered on these x, y, and z dimen-
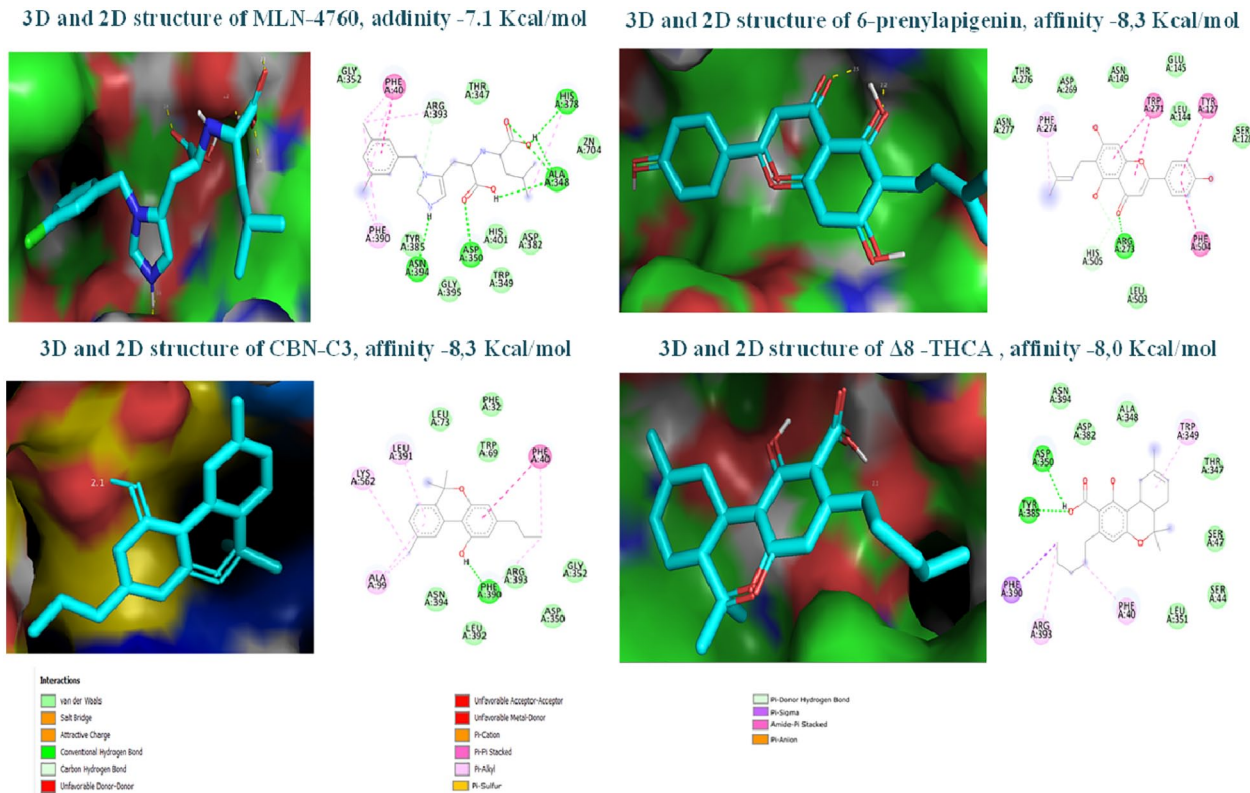
Figure 1. 3D and 2D structures of potential ligands derived from *Cannabis sativa* and MLN-4760 inhibitor of ACE2. All bond distances are from 2.2 to 2.4 Å. Top left: MLN-4760, top right: 6-prenylapigenin, down left: CBN-C3, and down right: Δ8-THCA. Δ8-THCA indicates Δ8-tetrahydrocannabinolic acid-A; CBN-C3, cannabivarin.

sions: center_x = 102.639879711, center_y = 0.477150403 941, center_z = 161.255542061, size_x = 73.0316322933, size_y = 74.5229742406, and size_z = 60.3917216095, with a flexibility of the atoms defined as the exhaustiveness equaling into 8.

Molecular visualization

The best pose of the compounds predicted with higher affinity and value scores was observed using PyMOL and DSV. The binding between ligands and the ACE2 active site and the images (Figure 1) were processed and visualized using the aforementioned tools DSV and PyMOL.

ADMET processing

The SwissADME server was used to predict molar refractivity, saturation, and promiscuity. The screening was performed using recognized medicinal chemistry criteria. The bioavailability allows for an initial assessment of a molecule's drug-likeness, and the Brain Or IntestinaL EstimateD permeation method (BOILED-Egg) model allows for intuitive evaluation of passive gastrointestinal absorption and brain penetration based on the position of the molecules by the function of lipophilicity WLOGP vs apparent polarity described by topological surface area (TPSA) referential plot. pkCSM was used to screen for chemical ADMET as the tools provide detailed attributes.

Results

Analysis of molecular docking scores and binding site of ACE2

Docking all 43 cannabinoid and noncannabinoid components of *C. sativa* with the ACE2 receptor identified 3 putative ligands with greater affinity to the receptor than its known inhibitor MLN-4760 (−7.1 kcal/mol as binding energy) and sharing nearly the same amino acid interaction. These top-scoring compounds are depicted in Figure 1. Their binding affinities to the active site of ACE2 are shown in Table 2. Angiotensin-converting enzyme II showed a significant interaction with hydrogen bonds to the following residues: ASP350 for both MLN-4760 and Δ8-THCA plus TYR385 for Δ8-THCA, and PHE390 for CBN-C3. 6-Prenylapigenin, CBN-C3, and Δ8-THCA obtained affinities of −8.3/−8.3/−8.0 kcal/mol, respectively (Table 2). From the point of view of binding energy, 6-prenylapigenin shows strong interactions with the target ACE2. From the hydrogen bond interactions, Δ8-THCA showed stronger than and similar binding residues to MLN-4760.

The ACE2 receptor adopts distinct conformations depending on whether it is bound by a ligand or a viral RBD, but the routes and mechanisms of ligand binding in the ACE2 receptor are unclear. In the context of SARS-CoV-2 and many other medical aspects, understanding the mechanism of ligand recognition by the ACE2 receptor is critical to building

Table 2. Molecular docking scores of the reference (MLN) and hit compounds from *C. sativa* with ACE2.

PUBCHEM ACCESSION ID	MOLECULE NAME	CHEMICAL CLASS	MOLECULAR FORMULA	ACE2 DOCKING SCORE (KCAL/MOL)
10382485	6-Prenylapigenin	Noncannabinoid (flavonoid)	$C_{20}H_{18}O_5$	−8.3
622545	Cannabivarin (CBN-C3)	Cannabinoid (cannabinol)	$C_{19}H_{22}O_2$	−8.3
59444391	Δ8-tetrahydrocannabinolic acid-A (Δ8-THCA)	Cannabinoid (Δ8-THC)	$C_{22}H_{30}O_4$	−8.0
448281	MLN-4760 (reference)	ACE2 inhibitor	$C_{19}H_{23}Cl_2N_3O_4$	−7.1

efficient antiviral medications. As shown in Figure 1, MLN-4760 docked with the ACE2 receptor had binding energy of −7.1 kcal/mol. The binding uses hydrogen bonds with Asp350, Ala348, His378, and Asn394, hydrophobic pi-pi stacked bonds with Phe40 and hydrophobic alkyl/pi-alkyl bonds with Phe40 and Phe390, and a carbon-hydrogen bond with Tyr385 (Figure 1).

6-Prenylapigenin has 1 conventional hydrogen bond at Arg273 and a pi-pi stacked bond with Tyr271, Tyr127, and Phe504. A pi-alkyl bond at Phe274 and finally a carbon-hydrogen bond at His505 are shown in Figure 1. For CBN-C3, 1 hydrogen bond at Phe390, a pi-pi stacked bond at Phe40, and a pi-alkyl bond with the following residues were observed: Leu391, Lys562, and Ala99. The last compound is Δ8-THCA, with Asp350, Tyr385 conventional hydrogen bonds, a pi-sigma with Phe390, and a pi-alkyl with Trp349, Phe40, and Arg393. All bonds were at a distance ranging from 2.1 to 2.6 Å (Figure 1).

Drug-likeness properties and other molecular descriptors of drug hits and reference compound

The drug-likeness features of the reference and hit compounds, such as hydrogen bond acceptor (HBA), hydrogen bond donor (HBD), log P, molecular weight, and TPSA, did not exceed 10, 5, 5, 500 g/mol and 140 Å, respectively (Figure 2 and Table 3). Furthermore, the reference and hit compound's molar refractivity ranged from 40 to 130, even though their number of rotatable bonds did not surpass 10 (Table 3).

ADMET properties of ligand hits and reference compound

The results shown in Table 4 disclose interesting results in which water solubility is greater than −6.0 log mol/L for all the ligands (reference and hits). The values for Cancer coli 2 (Caco-2) permeability (log Papp in 10^{-6} cm/s) were less than 0.9 for all but CBN-C3 (1.635). Intestinal absorption in humans was greater than 30% for all compounds, with Δ8-THCA being the highest (98.08%). Together with skin permeability, all compounds score under −2.5 (log Kp). Aside from 8-THCA, all compounds were found to be P-glycoprotein (Pgp) substrates. All compounds are not Pgp I and II inhibitors

aside from 6-prenylapigenin, which was predicted to be a Pgp II inhibitor only.

Moving onto the distribution, the volume of distribution steady-state value (log L/kg) was portrayed at more than 0.4 for 6-prenylapigenin and CBN-C3, although MLN-4760 and Δ8-THCA were 0.007 and −1.33, respectively. Regarding the blood-brain barrier (BBB), the permeability was less than 0.3 (log BB) for all compounds. The central nervous system (CNS) permeability (log PS) value was larger than −3.0 in MLN-4760 (−3.129).

Moreover, MLN-4760 and Δ8-THCA were not substrates for any cytochrome P450 nor inhibitors. Nevertheless, 6-prenylapigenin and CBN-C3 are substrates and inhibitors of most cytochrome P450 in addition to cytochrome P450 2D6.

In addition, for excretion, none of the compounds were substrates of renal organic cation transporter 2 (OCT2), and the total clearance ranged from −0.058 to 0.736 log mL/min/kg, with MLN-4760 being the lowest and Δ8-THCA being the highest. All compounds showed no dermotoxicity and were non inhibitors of human ether-a-go-go-related gene (hERG I) protein. Only MLN-4760 was predicted to be hepatotoxic, and CBN-C3 was *Salmonella typhimurium* reverse mutation assay (AMES) toxicity positive and hERG II inhibitor. The highest values for maximum tolerated dosage (log mg/kg/d), oral rat acute toxicity (LD50) (mol/kg), and oral rat chronic toxicity (log mg/kg/d) were found in MLN-4760 followed by Δ8-THCA. *Tetrahymena pyriformis* toxicity (log g/L) values for lead compounds and the reference were all greater than −0.5. For hazard and risk assessment in the aquatic environment, the Minnow toxicity was less than 0.3 for all the compounds.

Discussion

It has long been recognized that viral infections are difficult to treat, and phytochemicals have been used as antiviral agents against several viruses in view of the fact that they can inhibit viruses either at the viral entry point or during the replication stages, as well as through immunomodulation potentials.[19] Some plant constituents have the potential treatment and antiviral properties against SARS-CoV-2.[20]

COVID-19 infection is reliant on host cell factors, namely, ACE2. The strong attachment of virus spike (S) proteins to cell receptors allows CoVs to enter the host cell, enhancing viral entry and adhesion to the cell surface, which culminates in
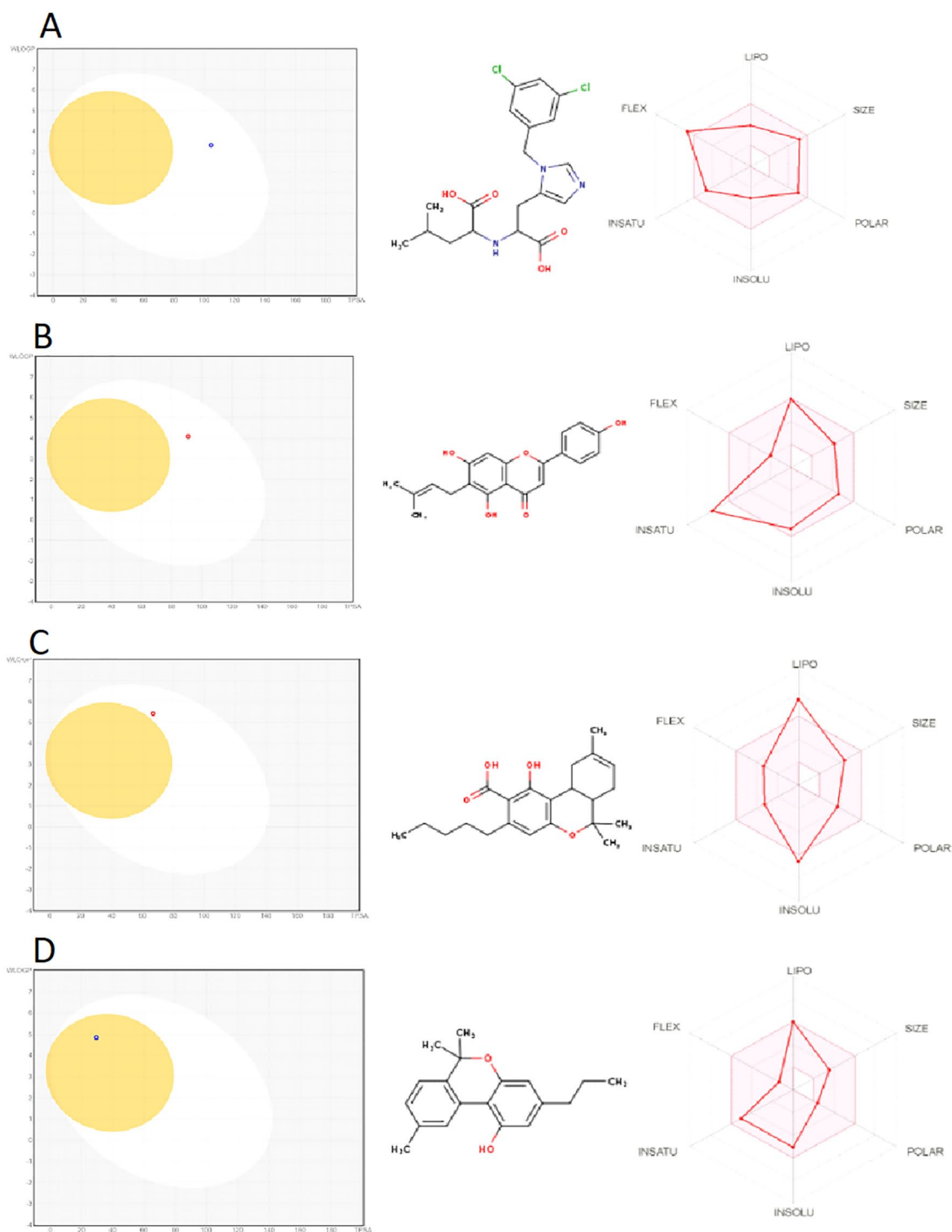
Figure 2. The bioavailability radars and BOILED-Egg for reference and hit compounds (A) MLN-4760 (reference), (B) 6-prenylapigenin, (C) Δ8-THCA, and (D) CBN-C3.

infection.[21] The major source of SARS-CoV-2 transmission was shown to be ACE2. As a result, the inhibitory action of effective metabolites on the ACE2 catalytic pocket may alter ACE2 conformation, inhibiting SARS-CoV-2 entrance into host cells.

Many studies have used molecular modeling to investigate the possibilities of countering COVID-19 infection using active ingredients obtained from natural sources. A recent in silico study[22] was conducted on certain cannabinoids using the SARS-CoV-2 Mpro (main protease) enzyme as the main target, followed by in vitro antiviral activity against SARS-CoV-2. Δ9-tetrahydrocannabinol and cannabidiol (CBD) showed the most significant antiviral potential, displaying IC50 values of 10.25 and 7.91 μM, respectively, which were comparable to those of lopinavir, chloroquine, and remdesivir, with IC50 values ranging between 8.16 and 13.15 μM.[22]

Table 3. Physiochemical properties of *C. sativa* hit compounds and reference.

DESCRIPTORS	MLN-4760 (REFERENCE)	6-PRENYLAPIGENIN	CBN-C3	Δ8-THCA
Molecular weight (g/mol)	428.31	338.35	282.38	358.47
Log P	2.06	3.59	4.50	5.05
Rotatable bonds	10	3	2	5
Hydrogen bond acceptors	6	5	2	4
Hydrogen bond donors	3	3	1	2
Molar refractivity	107.76	97.71	87.48	104.87
TPSA (Å)	104.45	90.90	29.46	66.76
Surface area	172.845	143.654	125.945	155.433

In this research, the cannabinoid and noncannabinoid components of *C. sativa* were examined in silico inside the binding pocket of ACE2. Our molecular docking analysis revealed that 6-prenylapigenin and CBN-C3 had the highest binding affinity with the lowest energy of –8.3 kcal/mol. This was followed by Δ8-THCA with an energy of –8.0 kcal/mol. Overall, all 3 drug affinity comparisons with the reference molecule MLN-4760, an inhibitor of ACE2, showed promising binding affinities.

A compound's drug-likeness is assessed qualitatively by the chance for a molecule to become an oral drug concerning bioavailability. It is determined by how similar a compound is to existing drugs in structural and physicochemical properties. The reference and hit compounds do not violate the physicochemical Ghose, Lipinski, and Veber rules, seeing that the values of their HBA, HBD, log P, molecular weight, TPSA, molar refractivity, and the number of rotatable bonds within the accepted range. However, for the pharmacophore point filter, the Mugge rule was not respected for Δ8-THCA and CBN-C3 with 1 violation, and XLOGP3 >5, which predicts the log P value using a known log P value of a reference compound as a starting point. To a large extent, they are all predicted to have good size, polarity, and flexibility, which positively correlate with good bioavailability.

However, the bioavailability radar of 6-prenylapigenin suggests that it is slightly unsaturated, with a fraction of carbons in the sp3 hybridization (Fsp3) valued at 0.15, which is less than 0.25. The bioavailability radar of Δ8-THCA suggests that the compound is poorly soluble and has low lipophilicity with an XLOGP3 higher than 5. Because drugs interact with a variety of molecular targets in the body, the biological activity profiles of potential drug candidates must account for human metabolism, and all hit compounds have strong enzyme inhibitory activity in bioactivity.

The ADMET characteristics of candidate compounds are the major reason for the high drug discovery attrition rates. Aqueous solubility is a key physicochemical attribute required for the characterization of an active pharmaceutical ingredient (API) during drug discovery.[23] Furthermore, with water solubility values less than –4.0 log mol/L, CBN-C3 is the only compound with poor solubility. The most convenient mode of drug delivery for medicines and xenobiotics is oral administration. The Caco-2 cell line is used in most specialized laboratories to screen novel chemical entities by predicting their solubility, bioavailability, and the probability of drug-drug or herb-drug interactions in the gut lumen because they closely resemble the human intestinal epithelium in many ways.[24] In our case, CBN-C3 showed the highest and Δ8-THCA the lowest in Caco-2 cell permeability. Along with Caco-2 permeability, all hit compounds have an excellent percentage of human intestinal absorption (HIA), with Δ8-THCA being the highest (98%). Skin permeability is undoubtedly effective, with a value of less than 2.5 log Kp. For all compounds, 6-prenylapigenin has the best dermal permeability value. P-glycoprotein acts as a transmembrane efflux pump, transporting substrates from the inside to the outside of the cell. It is one of the drug transporters responsible for the absorption and efflux of a variety of pharmaceuticals. All compounds are Pgp substrates aside from Δ8-THCA and 6-prenylapigenin, which was predicted to be a Pgp II inhibitor. This may promote the intracellular accumulation of substrates, resulting in potential human toxicity.

For the distribution part, the volume of distribution of steady state (VDSS) is low for all substrates, ranging from –1.33 to 0.615 L/kg, which is needed to maintain uniform distribution to give the same concentration in the plasma. As the fraction unbound in humans to which a drug binds to plasma proteins is low for all hits, in comparison to the reference, which exceeds 0.1, is by far the most available unbound (free) drug capable of interacting with a pharmacological target protein. The BBB is mainly maintained between –1.0 and 0.3. All hit compounds are moderately distributed in the brain, with Δ8-THCA predicted to have the best brain distribution although CBN-C3 has the poorest. Similarly, the reference compound MLN-4760 is unable to permeate the CNS, followed by 6-prenylapigenin.

Table 4. ADMET scores of hit compounds from *C. sativa* and the reference compound MLN-4760.

VARIABLES	MLN-4760 (REFERENCE)	6-PRENYLAPIGENIN	CBN-C3	Δ8-THCA
Absorption				
Solubility in water (log mol/L)	−2.892	−3.751	−5.174	−3.015
Permeabilities of Caco-2 (log Papp in 10^{-6} cm/s)	0.798	0.781	1.635	0.658
Intestinal absorption in humans (% absorbed)	44.973	92.307	93.168	98.08
Skin permeability (log Kp)	−2.735	−2.735	−2.689	−2.732
P-glycoprotein substrate (yes/no)	Yes	Yes	Yes	No
P-glycoprotein I inhibitor (yes/no)	No	No	No	No
P-glycoprotein II inhibitor (yes/no)	No	Yes	No	No
Distribution				
Volume of distribution steady-state in humans (log L/kg)	0.007	0.426	0.615	−1.33
Fraction unbound in human (Fu)	0.382	0.037	0	0.107
BBB permeability (log BB)	−1.369	−1.026	0.646	−0.124
CNS permeability (log PS)	−3.129	−1.992	−1.62	−1.948
Metabolism				
Substrate of cytochrome P450 2D6 (yes/no)	No	No	No	No
Substrate of cytochrome P450 3A4 (yes/no)	No	Yes	Yes	No
Inhibitor of cytochrome P450 1A2 (yes/no)	No	Yes	Yes	No
Inhibitor of cytochrome P450 2C19 (yes/no)	No	Yes	Yes	No
Inhibitor of cytochrome P450 2C9 (yes/no)	No	Yes	Yes	No
Inhibitor of cytochrome P450 2D6 (yes/no)	No	No	No	No
Inhibitor of cytochrome P450 3A4 (yes/no)	No	Yes	Yes	No
Excretion				
Total clearance (log mL/min/kg)	−0.058	0.358	0.725	0.736
Renal OCT2 substrate (yes/no)	No	No	No	No
Toxicity				
AMES toxicity (yes/no)	No	No	Yes	No
Maximum tolerated dose in humans (log mg/kg/d)	0.445	0.265	0.357	0.38
hERG I inhibitor (yes/no)	No	No	No	No
hERG II inhibitor (yes/no)	No	No	Yes	No
Oral rat acute toxicity (LD50) (mol/kg)	2.483	2.481	2.063	2.684
Oral rat chronic toxicity (LOAEL) (log mg/ky_bw/d)	2.429	1.437	1.654	1.878
Hepatotoxicity (yes/no)	Yes	No	No	No
Skin sensitization (yes/no)	No	No	No	No
T. Pyriformis toxicity (log μg/L)	0.285	0.414	1.347	0.286
Minnow toxicity (log mM)	1.691	1.241	−0.222	−0.353

Abbreviations: Δ8-THCA indicates Δ8-tetrahydrocannabinolic acid-A; AMES, *Salmonella typhimurium* reverse mutation assay; BBB, blood-brain barrier; Caco-2, Cancer coli 2 (human colorectal adenocarcinoma cells); CBN-C3, cannabivarin, CNS, central nervous system; hERG, human ether-a-go-go-related gene; LOAEL, lowest observed adverse effect level; OCT2, organic cation transporter 2; *T. pyriformis: Tetrahymena pyriformis*.

Metabolism-wise, cytochrome P450 is responsible for the biotransformation of most drugs and is a primary cause of variability in drug pharmacokinetics. Strikingly, 6-prenylapigenin and CBN-C3 are substrates of cytochrome P450 3A4 and inhibitors of CYP P450 1A2, 2C19, 2C9, and 3A4, causing the accumulation of the substrates of these enzymes.

The total clearance of a drug from the bloodstream is the sum of renal clearance plus hepatic clearance plus clearance from all other tissues.[25] The renal OCT2 of all hit compounds will not be carried out from plasma into the cells by renal OCT2 and will also have no deleterious interaction when coadministered with renal OCT2 inhibitors.

The toxicity of a molecule is one of the most important aspects of drug and lead propositions; AMES toxicity was detected in the CBN-C3 compound only, which is also an hERG II inhibitor. The maximum tolerated dose in humans is mostly kept at less than 0.477 log (mg/kg/d), which they all attain. We can also observe that Δ8-THCA is the safest in acute toxicity (LD50) and MLN-4760 for chronic toxicity (lowest observed adverse effect level [LOAEL]). Similarly, MLN-4760 is the safest for the Minnow toxicity, and CBN-C3 is the safest for *T pyriformis* toxicity. In the matter of hepatotoxicity, all lead compounds were found to be nonhepatotoxic and nondermo toxic.

There has not been much study done on the 6-prenylapigenin chemical, but it showed moderate anti-methicillin-resistant *Staphylococcus aureus* (anti-MRSa) (IC50 = 6.5 μg/mL), weak anticandidal (IC50 = 20.0 μg/mL) and mild antimalarial activity against the *Plasmodium falciparum* D6 clone and W2 clone with IC50 values of 2.8 and 2.0 μg/mL, respectively.[26] It was also shown that it inhibited melanin biosynthesis in B16 melanoma cells and showed antioxidant and antitrichomonal activities.[27]

Cannabivarin (CBN-C3) was identified in 1969 by Vollner *et al*[28] as a CBD homolog in which the side chain is C3H7 instead of C5H11.[29] Δ8-tetrahydrocannabinolic acid-A is an analog of tetrahydrocannabinol (THC) with antiemetic, anxiolytic, appetite-stimulating, analgesic, and neuroprotective properties.[30] It is chemically and functionally similar to Δ-9-tetrahydrocannabinol (Δ9-THC), producing similar physiological and toxicological effects.

As previously stated, ACE2 is an important component of the RAS. Angiotensin-converting enzyme II inhibits the activation of the RAS ACE-angiotensin II (Ang II)-angiotensin type 1 receptor (AT1R) axis and protects the lungs from damage. The same is true for 2019-nCoV, which employs ACE2 for cell entrance.[31] Targeting the spike protein may be a wise choice to contain the virus and may have a positive impact as we do not tamper with human ACE2's natural function, as shown in a study,[32] in which they discovered that cannabigerolic acid and cannabidiolic acid were equally effective against the 2 SARS-CoV-2 variants alpha B.1.1.7 and beta B.1.351. These compounds are orally

bioavailable and have a long history of safe human use. However, we chose to target the ACE2 because many studies have shown that ACE inhibitors, as well as angiotensin-receptor blockers (ARBs) used either alone or in combination, can be ideal to boost immune responses while also reducing inflammation and organ damage associated with COVID-19 symptoms.[33]

The syndrome of acute respiratory distress (ARDS) is a clinically life-threatening condition induced by the excessive activation of RAS triggered by 2019-nCoV infection, and ACE2 protects against COVID-19-induced ARDS.[31] Because of ACE2's ARDS-protective properties, the development of drugs enhancing ACE2 activity may become one of the most promising approaches for the treatment of COVID-19 in the near future. Meanwhile, RAS medications such as ACE inhibitors and angiotensin II receptor blockers of the RAS cascade in the lung may be favorable.

Many other investigations, most notably Wang *et al*,[34] deployed a gene modulation strategy demonstrating *ACE2* gene expression modulation using *C. sativa* extracts. Cannabidiol has been demonstrated to alter gene expression and inflammation, and have anti-inflammatory and anticancer properties. Several *C. sativa* extracts reduce the gene expression of *TMPRSS2*, another key protein for SARS-CoV-2 entry into host cells.

Our experiment suggests novel chemical components of *C. sativa* that could be used as therapeutic molecules against COVID-19. It was designed to test novel cannabis extracts for their ability to prevent spike interaction with ACE2 target, employing ACE2 blockade as an analysis strategy. Finally, our investigation incorporated both cannabinoid and noncannabinoid components of *C. sativa*. This enables us to highlight the significant impacts of cannabis on ACE2 blockage. Further investigations are being pursued, namely, molecular dynamics and quantitative structure-activity relationship (QSAR) studies, to refine these findings and to correlate the exact activity of the hits with ACE2 and inflammation as well as its outcome.

Conclusions

With hit identification of the components of *C. sativa*, docking combined with a scoring function can be used to quickly screen our databases of potential drugs in silico and to identify molecules that are likely to bind to the protein target ACE2 of interest; hence, inhibiting the interaction between the viral RBD and host ACE2 presents a promising strategy for blocking SAR-COV-2 entry into human cells and also upregulating ACE2 expression. Listing hit compounds may be capable of forming a closed shape of ACE2 restricting access to the spike S protein and limiting SARS-CoV-2 infections. Our research reveals that 6-prenylapigenin, CBN-C3, and 8-THCA are 3 compounds that have shown promising binding and drug-likeness outcomes, which should be evaluated further for pharmaceutical development research.

REFERENCES

1. Tao Q, Du J, Li X, et al. Network pharmacology and molecular docking analysis on molecular targets and mechanisms of Huashi Baidu formula in the treatment of COVID-19. *Drug Dev Ind Pharm*. 2020;46:1345-1353. doi:10.1080/03639045.2020.1788070.

2. Li W, Moore MJ, Vasilieva N, et al. Angiotensin-converting enzyme 2 is a functional receptor for the SARS coronavirus. *Nature*. 2003;426:450-454. doi:10.1038/nature02145.

3. Warner FJ, Smith AI, Hooper NM, Turner AJ. Angiotensin-converting enzyme-2: a molecular and cellular perspective. *Cell Mol Life Sci*. 2004;61:2704-2713. doi:10.1007/s00018-004-4240-7.

4. Burrell LM, Johnston CI, Tikellis C, Cooper ME. ACE2, a new regulator of the renin-angiotensin system. *Trends Endocrinol Metab*. 2004;15:166-169. doi:10.1016/j.tem.2004.03.001.

5. Nami B, Ghanaeian A, Ghanaeian K, Nami N. The effect of ACE2 inhibitor MLN-4760 on the interaction of SARS-CoV-2 spike protein with human ACE2: a molecular dynamics study [published online ahead of print April 22, 2020]. doi:10.26434/chemrxiv.12159945.v1.

6. Kriese U, Schumann E, Weber WE, Beyer M, Brühl L, Matthäus. Oil content, tocopherol composition and fatty acid patterns of the seeds of 51 *Cannabis sativa L*. genotypes. *Euphytica*. 2004;137:339-351. doi:10.1023/B:EUPH.0000040473.23941.76.

7. Stambouli H, El Bouri A, Bellimam MA, Bouayoun T, El Karni N. Cultivation of *Cannabis sativa L* in northern Morocco. *Bull Narc*. 2005;57:79-118.

8. Elsohly M, Gul W. Constituents of *Cannabis sativa*. *Adv Exp Med Biol*. 2014;1264:3-22. doi:10.1093/acprof:oso/9780199662685.003.0001.

9. Elsohly MA, Slade D. Chemical constituents of marijuana: the complex mixture of natural cannabinoids. *Life Sci*. 2005;78:539-548. doi:10.1016/j.lfs.2005.09.011.

10. Turner CE, Elsohly MA, Boeren EG. Constituents of *Cannabis sativa L*. XVII: a review of the natural constituents. *J Nat Prod*. 1980;43:169-234. doi:10.1021/np50008a001.

11. Bhattarai A, Pawnikar S, Miao Y. Mechanism of ligand recognition by human ACE2 receptor. *Biorxiv Prepr Serv Biol*. 2021;12:4814-4822. doi:10.1101/2020.10.30.362749.

12. Towler P, Staker B, Prasad SG, et al. ACE2 X-ray structures reveal a large hinge-bending motion important for inhibitor binding and catalysis. *J Biol Chem*. 2004;279:17996-18007. doi:10.1074/jbc.M311191200.

13. Schrödinger L. The PyMOL molecular graphics system. Version 1.3r1.

14. DSV. *BIOVIA discovery studio visualizer*. Vélizy-Villacoublay: Dassault Systemes.

15. Daina A, Michielin O, Zoete V. SwissADME: a free web tool to evaluate pharmacokinetics, drug-likeness and medicinal chemistry friendliness of small molecules. *Sci Rep*. 2017;7:42717. https://www.nature.com/articles/srep42717. Accessed August 23, 2022.

16. Pires DEV, Blundell TL, Ascher DB. pkCSM: predicting small-molecule pharmacokinetic and toxicity properties using graph-based signatures. *J Med Chem*. 2015;58:4066-4072. https://pubs.acs.org/doi/10.1021/acs.jmedchem.5b00104. Accessed August 23, 2022.

17. Morris GM, Huey R, Lindstrom W, et al. AutoDock4 and AutoDockTools4: automated docking with selective receptor flexibility. *J Comput Chem*. 2009;30:2785-2791. doi:10.1002/jcc.21256.

18. Dallakyan S, Olson AJ. Small-molecule library screening by docking with PyRx. *Methods Mol Biol*. 2015;1263:243-250. doi:10.1007/978-1-4939-2269-7_19.

19. Anand AV, Balamuralikrishnan B, Kaviya M, et al. Medicinal plants, phytochemicals, and herbs to combat viral pathogens including SARS-CoV-2. *Mol Basel Switz*. 2021;26:1775. doi:10.3390/molecules26061775.

20. Adhikari B, Marasini BP, Rayamajhee B, et al. Potential roles of medicinal plants for the treatment of viral diseases focusing on COVID-19: a review. *Phytother Res*. 2021;35:1298-1312. doi:10.1002/ptr.6893.

21. Hoffmann M, Kleine-Weber H, Schroeder S, et al. SARS-CoV-2 cell entry depends on ACE2 and TMPRSS2 and is blocked by a clinically proven protease inhibitor. *Cell*. 2020;181:271.e-280.e8. doi:10.1016/j.cell.2020.02.052.

22. Raj V, Park JG, Cho KH, et al. Assessment of antiviral potencies of cannabinoids against SARS-CoV-2 using computational and in vitro approaches. *Int J Biol Macromol*. 2021;168:474-485. doi:10.1016/j.ijbiomac.2020.12.020.

23. Elder D, Holm R. Aqueous solubility: simple predictive methods (in silico, in vitro and bio-relevant approaches). *Int J Pharm*. 2013;453:3-11. doi:10.1016/j.ijpharm.2012.10.041.

24. Awortwe C, Fasinu PS, Rosenkranz B. Application of Caco-2 cell line in herb-drug interaction studies: current approaches and challenges. *J Pharm Pharm Sci*. 2014;17:1-19. doi:10.18433/j30k63.

25. Horde GW, Gupta V. Drug clearance. In: *Statpearls*. Statpearls Publishing; 2022. http://www.ncbi.nlm.nih.gov/books/NBK557758/. Accessed August 23. 2022.

26. Radwan MM, Elsohly MA, Slade D, et al. Non-cannabinoid constituents from a high potency *Cannabis sativa* variety. *Phytochemistry*. 2008;69:2627-2633. doi:10.1016/j.phytochem.2008.07.010.

27. Kuete V, Ngameni B, Wiench B, et al. Cytotoxicity and mode of action of four naturally occuring flavonoids from the genus Dorstenia: gancaonin Q, 4-hydroxylonchocarpin, 6-prenylapigenin, and 6,8-diprenyleriodictyol. *Planta Med*. 2011;77:1984-1989. doi:10.1055/s-0031-1280023.

28. Vollner L, Bieniek D, Korte F. [Hashish. XX. Cannabidivarin, a new Hashish constituent]. *Tetrahedron Lett*. 1969;145-147. doi:10.1016/s0040-4039(01)87494-3.

29. Merkus FW. Cannabivarin and tetrahydrocannabivarin, two new constituents of hashish. *Nature*. 1971;232:579-580. doi:10.1038/232579a0.

30. Definition of delta-8-tetrahydrocannabinol-NCI, drug dictionary-NCI. https://www.cancer.gov/publications/dictionaries/cancer-drug/def/delta-8-tetrahydrocannabinol. Published February 2, 2011. Accessed August 23, 2022.

31. Zhang X, Li S, Niu S. ACE2 and COVID-19 and the resulting ARDS. *Postgrad Med J*. 2020;96:403-407. doi:10.1136/postgradmedj-2020-137935.

32. van Breemen RB, Muchiri RN, Bates TA, et al. Cannabinoids block cellular entry of SARS-CoV-2 and the emerging variants. *J Nat Prod*. 2022;85:176-184. doi:10.1021/acs.jnatprod.1c00946.

33. Chatterjee B, Thakur SS. ACE2 as a potential therapeutic target for pandemic COVID-19. *RSC Adv*. 2020;10:39808-39813. doi:10.1039/D0RA08228G.

34. Wang B, Kovalchuk A, Li D, et al. In search of preventive strategies: novel high-CBD *Cannabis sativa* extracts modulate ACE2 expression in COVID-19 gateway tissues. *Aging*. 2020;12:22425-22444. doi:10.18632/aging.202225.